

## Study of the $^{242}\text{Pu}(d, t)^{241}\text{Pu}$ and $^{242}\text{Pu}(^3\text{He}, \alpha)^{241}\text{Pu}$ Reactions\*

Th. W. Elze and J. R. Huizenga

*Nuclear Structure Research Laboratory and Departments of Chemistry and Physics,  
University of Rochester, Rochester, New York 14627*

(Received 28 August 1970)

Energy levels of  $^{241}\text{Pu}$  have been studied through the  $^{242}\text{Pu}(d, t)$  and  $^{242}\text{Pu}(^3\text{He}, \alpha)$  reactions induced by 17-MeV deuterons and 30-MeV  $^3\text{He}$  particles, respectively. Transferred orbital angular momenta are obtained from  $(^3\text{He}, \alpha)$  angular distributions and from cross-section ratios  $R = d\sigma(^3\text{He}, \alpha)/d\sigma(d, t)$ . The ratios  $R$  vary by a factor of  $10^3$  for a change in  $l$  from 0 to 7 and provide a very sensitive measure of the angular momentum transfer. Experimentally measured spectroscopic factors are found to be in reasonable agreement with those calculated from Nilsson wave functions. Rotational bands associated with the following Nilsson configurations are identified in  $^{241}\text{Pu}$ :  $\frac{5}{2}^+[622]$ ,  $\frac{7}{2}^+[624]$ ,  $\frac{1}{2}^+[631]$ ,  $\frac{7}{2}^- [743]$ ,  $\frac{3}{2}^+[631]$ ,  $\frac{1}{2}^- [501]$ , and  $\frac{5}{2}^- [752]$ .

### I. INTRODUCTION

The one-nucleon transfer reaction has been shown<sup>1</sup> to be a useful tool for the study of heavy deformed nuclei. In the framework of the Nilsson model, the distribution of differential cross sections to levels within a rotational band depends on the wave function of the intrinsic state on which the band is based, and this feature has been used to make Nilsson-state assignments. In the actinide region of the Periodic Table, several nuclei have been studied by  $(d, p)$  and  $(d, t)$  reactions,<sup>2</sup> as well as by  $^3\text{He}$  and  $\alpha$ -induced reactions.<sup>3,4</sup>

In the present work we have studied the  $(d, t)$  and  $(^3\text{He}, \alpha)$  neutron-pickup reactions leading to levels of  $^{241}\text{Pu}$ . The information obtained from each of these reactions is complementary in that the  $(^3\text{He}, \alpha)$  process, because of the big momentum mismatch involved, favors high-angular-momentum transfers while the  $(d, t)$  reaction transfers predominantly lower angular momenta. This disparity in angular momentum transfer affords one a means of determining  $l$  values by comparison of the strengths of corresponding groups observed in both spectra.

The level scheme of  $^{241}\text{Pu}$  had previously been studied by  $\alpha$  decay<sup>5,6</sup> of  $^{245}\text{Cm}$  and subsequent emission of  $\gamma$  radiation, and, more recently, by a  $(d, p)$ -reaction experiment.<sup>2</sup> On the basis of these measurements, a few rotational levels were identified and Nilsson-state assignments made. However, several neutron-hole excitations and associated rotational bands expected in  $^{241}\text{Pu}$  from the Nilsson model were still undiscovered. The  $(d, t)$  and  $(^3\text{He}, \alpha)$  pickup reactions are especially well suited to excite these hitherto unseen states. We therefore studied the  $^{242}\text{Pu}(d, t)^{241}\text{Pu}$  and  $^{242}\text{Pu}(^3\text{He}, \alpha)^{241}\text{Pu}$  reactions. Preliminary results have been reported.<sup>7</sup>

### II. EXPERIMENTAL PROCEDURE AND RESULTS

Beams of 17-MeV deuterons and 30-MeV- $^3\text{He}$  particles for the present measurements were obtained from the Emperor Tandem Van de Graaff accelerator of the University of Rochester. The target<sup>8</sup> consisted of a  $1 \times 5\text{-mm}^2$   $\text{PuO}_2$  strip, enriched to 99.8%  $^{242}\text{Pu}$ , deposited on a  $20\text{-}\mu\text{g}/\text{cm}^2$  carbon backing. The thickness of the target material was about  $50\text{ }\mu\text{g}/\text{cm}^2$ . Triton and  $\alpha$  spectra from the  $(d, t)$  and  $(^3\text{He}, \alpha)$  reactions, respectively, were analyzed with an Enge split-pole magnetic spectrograph and detected with nuclear emulsion plates. Spectra were recorded at a laboratory angle of  $60^\circ$ . Additional shorter exposures of the  $(^3\text{He}, \alpha)$  reaction were made at  $25^\circ$ ,  $35^\circ$ , and  $90^\circ$  in order to obtain angular distributions of the stronger  $\alpha$  groups. A scintillation counter mounted at  $45^\circ$  to the beam direction monitored the  $^3\text{He}$  particles and deuterons elastically scattered from the target. The output of this detector served for intensity normalization of the individual spectra and for the determination of absolute reaction cross sections. For the latter purpose, the elastic-scattering cross section for 30-MeV- $^3\text{He}$  particles on  $^{242}\text{Pu}$  was taken to be equal to the Rutherford cross section, as predicted by distorted-wave Born-approximation (DWBA) calculations and confirmed in a separate measurement. Since no experimental data on elastic scattering cross sections for deuterons were available, absolute  $(d, t)$  intensities were determined with the stipulation that best over-all agreement between  $(d, t)$  and  $(^3\text{He}, \alpha)$  spectroscopic factors was achieved. Reversing the calibration procedure used for the  $(^3\text{He}, \alpha)$  reaction, the deuteron elastic scattering cross section was then calculated from the absolute  $(d, t)$  intensities and compared with the DWBA prediction. Agreement of better than 5% was found giving added confidence in the

absolute  $(d, t)$  cross sections as measured in the present experiment.

In Fig. 1, the triton and  $\alpha$  spectra measured at a lab angle of  $60^\circ$  are shown. The excitation energies and reaction cross sections of the observed levels of  $^{241}\text{Pu}$  are listed in Table I. The energy values shown here are averages from the  $(d, t)$  and  $(^3\text{He}, \alpha)$  experiments. Absolute cross sections are believed to be accurate to within 20%. Table I also contains the proposed assignments resulting from the analysis discussed below. A partial level scheme of  $^{241}\text{Pu}$  as obtained by combining our results with previously published data<sup>2, 5, 6</sup> is shown in Fig. 2. Levels indicated by heavy lines are observed in the present experiment. Assigned states seen in previous works but not observed in our experiment are drawn as thinner lines. Levels belonging to rotational bands that are not excited by the pickup reaction are not included. The energies of the  $\frac{1}{2}^+[631\uparrow]$  and  $\frac{3}{2}^+[631\downarrow]$  levels quoted in Fig. 2

are taken from Ref. 2, since these levels are not resolved in the present experiment.

### III. ANALYSIS AND DISCUSSION

As a first step in the analysis of the spectra shown in Fig. 1, the triton and  $\alpha$  groups are associated with known levels on the basis of an energy fit. Nilsson configurations are then assigned by comparison of experimental and calculated spectroscopic factors.

The differential cross section for a one-nucleon pickup reaction on an even, deformed target nucleus may be written<sup>1</sup>

$$(\frac{d\sigma}{d\Omega})_{0 \rightarrow I_f = j} = 2Nc_{j_l}^2 V^2 \sigma_l(\theta, Q). \quad (1)$$

In this expression,  $\sigma_l(\theta, Q)$  is the intrinsic single-particle cross section for pickup of a neutron with orbital angular momentum  $l$ ,  $N$  is a normalization constant, and the quantity  $S = 2c_{j_l}^2 V^2$  is the spectroscopic factor which contains all the nuclear-structure information on the state excited by the reaction.

Calculations of the  $\sigma_l(\theta, Q)$  utilized the DWBA<sup>9</sup> computer code DWUCK.<sup>10</sup> The optical-model parameters<sup>11, 12</sup> used in the present calculations are shown in Table II. Spin-orbit effects and finite-range corrections have not been included. The  $\sigma_l(\theta, Q)$  were calculated for  $Q$  values corresponding to excitation energies of 0 and 1 MeV, with linear interpolation used to find the cross sections for the appropriate excitation energies. Normalization factors  $N$  of 25 and 3.33 were used for the  $(^3\text{He}, \alpha)$ <sup>13</sup> and  $(d, t)$ <sup>14</sup> reactions, respectively.

Assignments of  $l$  values to the observed transitions are based on  $(^3\text{He}, \alpha)$  angular distributions and cross-section ratios  $R = d\sigma(^3\text{He}, \alpha)/d\sigma(d, t)$ . Angular distributions of three strong  $\alpha$  groups measured in the  $(^3\text{He}, \alpha)$  reaction are shown in Fig. 3. The solid curves are the results of the DWBA calculations. Although quite good fits were achieved, it was extremely difficult to make definite  $l$  assignments from these angular distributions. More reliable information on transferred angular momenta is obtained from an analysis of the aforementioned cross-section ratios  $R$ . Since the  $l$  dependence of  $(^3\text{He}, \alpha)$  and  $(d, t)$  cross sections is quite different, as was outlined in Sec. I, the cross-section ratio  $R$  provides a more sensitive indication of the  $l$  values than angular distributions. DWBA calculations give evidence that the ratio  $R$  increases by about a factor of  $10^3$  as  $l$  varies from 0 to 7. In Table III, experimentally measured cross-section ratios are compared with calculated ones. The sensitivity of the cross-section ratio  $R$  to the transferred angular momentum  $l$  can be judged from the last three columns of Ta-

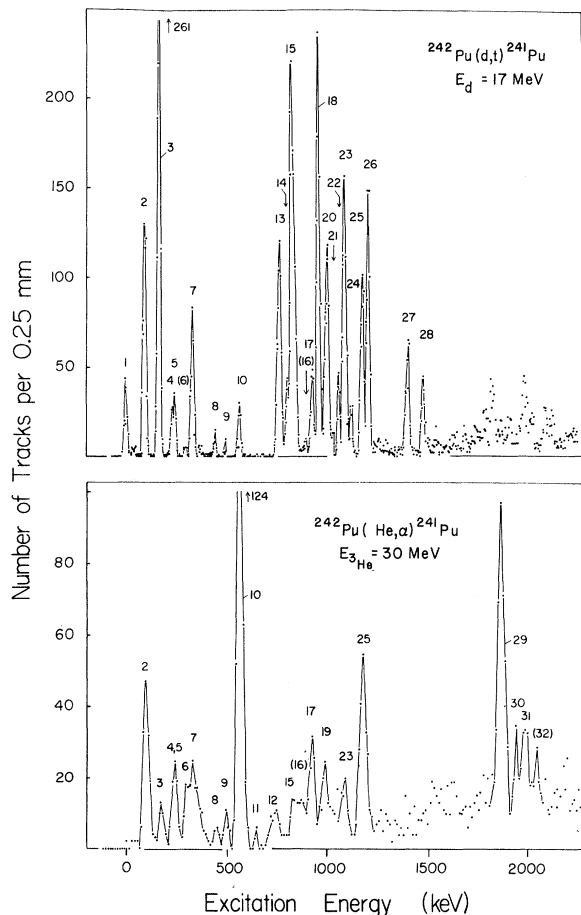


FIG. 1. Triton and  $\alpha$  spectra from the  $^{242}\text{Pu}(d, t)$  and  $^{242}\text{Pu}(^3\text{He}, \alpha)$  reactions, respectively, measured at  $\theta_{\text{lab}} = 60^\circ$ . The numbers labeling the individual lines correspond to those given in Table I.

TABLE I. Levels of  $^{241}\text{Pu}$  excited by the  $^{242}\text{Pu}(^3\text{He},\alpha)$  and/or  $^{242}\text{Pu}(d,t)$  reaction.

Line	Excitation energy (keV)	$d\sigma(60^\circ)/d\Omega$ ( $\mu\text{b/sr}$ )		Assignment
		$(^3\text{He},\alpha)$	$(d,t)$	
1	0		$68 \pm 14$	$\frac{5}{2}^+$ [622 $\uparrow$ ]
2	$92 \pm 2$	$10 \pm 2$	$280 \pm 28$	$\frac{9}{2}^+$ [622 $\uparrow$ ]
3	$167 \pm 3$	$3.0 \pm 0.6$	$520 \pm 68$	$\left\{ \begin{array}{l} \frac{1}{2}^+ + \frac{3}{2}^+ [631\downarrow] + \\ \frac{11}{2}^+ [622\uparrow] \end{array} \right.$
4	$235 \pm 4$	$5.7 \pm 0.8$	$48 \pm 12$	$\frac{5}{2}^+ [631\downarrow] + \frac{13}{2}^+ [622\uparrow]$
5	$244 \pm 4$		$45 \pm 11$	
6	(296)	$3.8 \pm 0.9$	$\approx 5$	$\frac{11}{2}^+$ [624 $\downarrow$ ]
7	$334 \pm 3$	$5.0 \pm 0.9$	$144 \pm 15$	$\frac{9}{2}^+$ [631 $\downarrow$ ]
8	$444 \pm 3$	$1.3 \pm 0.4$	$18 \pm 4$	$\frac{11}{2}^-$ [743 $\downarrow$ ]
9	$499 \pm 3$	$1.8 \pm 0.5$	$\approx 5$	$\frac{13}{2}^+$ [631 $\downarrow$ ]
10	$568 \pm 2$	$28 \pm 2$	$45 \pm 8$	$\frac{15}{2}^-$ [743 $\downarrow$ ]
11	$645 \pm 9$	$\approx 0.5$		
12	$752 \pm 6$	$2.1 \pm 0.6$		
13	$775 \pm 3$		$233 \pm 24$	
14	$809 \pm 3$		$\approx 80$	$(\frac{3}{2}^+ [631\uparrow])$
15	$835 \pm 3$	$\approx 3.4$	$423 \pm 51$	$(\frac{5}{2}^+ [631\uparrow])$
(16)	(875)	$(\approx 3.3)$	$(\approx 19)$	$(\frac{7}{2}^+ [631\uparrow])$
17	$931 \pm 2$	$6.8 \pm 0.9$	$107 \pm 10$	$(\frac{9}{2}^+ [631\uparrow])$
18	$967 \pm 3$		$440 \pm 60$	$\frac{1}{2}^-$ [501 $\downarrow$ ]
19	$994 \pm 3$	$5 \pm 2$		$(\frac{11}{2}^+ [631\uparrow])$
20	$1009 \pm 2$		$219 \pm 28$	$\frac{3}{2}^- + \frac{5}{2}^-$ [501 $\downarrow$ ]
(21)	( $\approx 1030$ )		( $\approx 23$ )	
22	$1060 \pm 4$		$108 \pm 22$	
23	$1090 \pm 2$	$3.6 \pm 0.7$	$318 \pm 32$	
24	$1121 \pm 4$		$57 \pm 16$	
25	$1181 \pm 3$	$11 \pm 2$	$172 \pm 28$	$\frac{9}{2}^+$ [633 $\downarrow$ ]?
26	$1211 \pm 3$		$310 \pm 31$	
27	$1402 \pm 3$		$117 \pm 16$	
28	$1473 \pm 3$		$78 \pm 15$	
29	$1868 \pm 5$	$20 \pm 3$		$\frac{15}{2}^-$ [752 $\downarrow$ ]
30	$1944 \pm 5$	$4.2 \pm 0.9$		
31	$1991 \pm 4$	$6 \pm 1$		
(32)	( $\approx 2045$ )	( $\approx 3$ )		

ble III in which the theoretical  $R$  is listed for three neighboring  $l$  values,  $l_0 - 1$ ,  $l_0$ ,  $l_0 + 1$ , where  $l_0$  denotes the orbital angular momentum assigned to the transition. For most of the levels listed in Table III,  $l$  values were determined unambiguously from these cross-section ratios  $R$ .

Spectroscopic factors  $S = 2c_{ji}^2 V^2$  were calculated from Nilsson wave functions. Here, the coefficient  $c_{ji}$  results from the expansion of the deformed state in terms of basis states of definite  $l$  and  $j$ , e.g.,  $|N\Omega\rangle = \sum_{ji} c_{ji} |Njl\Omega\rangle$ . In the present work, the calculation of spectroscopic factors employed the

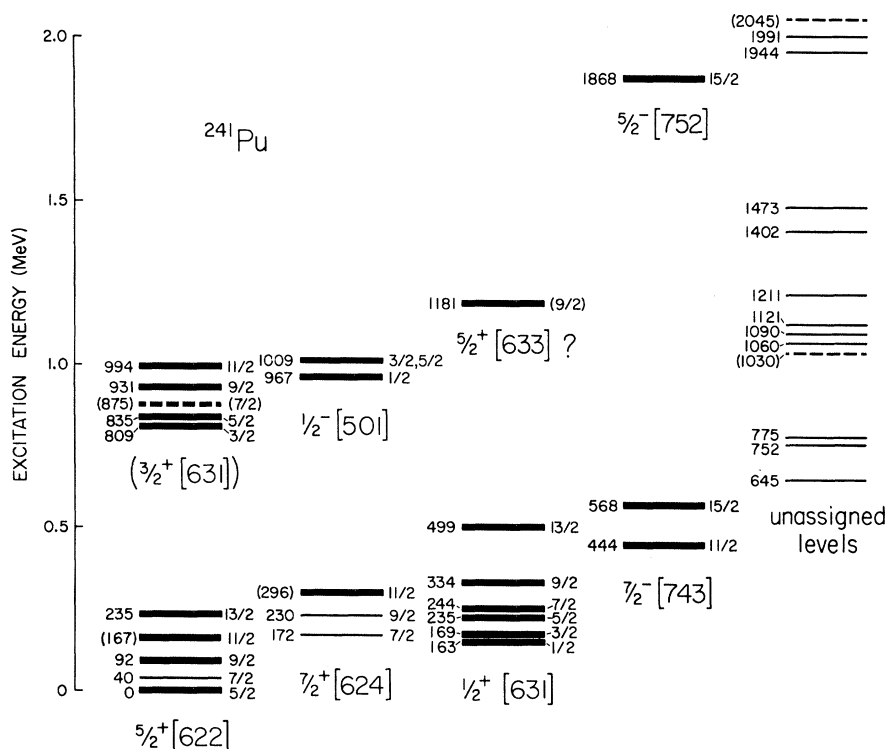


FIG. 2. Partial level scheme of  $^{241}\text{Pu}$  as obtained with the present results and previously published data. Assigned states observed in the present experiment are drawn as heavy lines, states seen in previous experiments as thinner lines.

$c_{ji}$  coefficients tabulated by Chi.<sup>15</sup> A quadrupole deformation of  $\beta = 0.25$  was used for  $^{241}\text{Pu}$ . The factor  $V^2$  is the neutron-occupation probability for the state excited by the reaction. Approximate values of  $V^2$  were estimated from pairing theory<sup>16</sup> by fitting measured excitation energies to theoretical quasiparticle energies of the  $5/2^+$  [622 $\uparrow$ ],  $7/2^+$  [624 $\uparrow$ ], and  $1/2^+$  [631 $\uparrow$ ] states.

A comparison of theoretical spectroscopic factors with those observed in the  $(d, t)$  and  $(^3\text{He}, \alpha)$  reactions is shown in Table IV. Only rotational states with spins  $J \leq N + \frac{1}{2}$  are listed in this table, since the simple Nilsson model used here predicts vanishing spectroscopic factors for all higher-spin

states. Band mixing has been neglected in the calculations. For most of the states listed in Table IV satisfactory agreement between calculated and observed spectroscopic factors is obtained. Levels belonging to the [501 $\uparrow$ ], [743 $\uparrow$ ], and [633 $\uparrow$ ] bands, however, have spectroscopic factors that deviate strongly from the theoretical values.

The [622 $\uparrow$ ], [624 $\uparrow$ ], and [631 $\uparrow$ ] configurations were previously assigned in  $^{241}\text{Pu}$  from radioactive-decay<sup>5,6</sup> and  $(d, p)$ -reaction<sup>2</sup> studies. The spectroscopic factors obtained from the present experiment confirm these assignments. The generally good agreement between theoretical and experimental spectroscopic factors indicates that the levels

TABLE II. Optical-model parameters. The optical potential used has the form  $U(r) = -V(1 + e^X)^{-1} - i[W - 4W_D(d/dX)'] \times (1 + e^X)^{-1}$ , where  $X = (r - r_0 A^{1/3})/a$ , and  $X' = (r - r_0' A^{1/3})/a'$ . The Coulomb potential used is due to a uniformly charged sphere of radius  $R_C = r_C A^{1/3}$ .

	$V$ (MeV)	$r_0$ (fm)	$a$ (fm)	$W$ (MeV)	$W_D$ (MeV)	$r_0'$ (fm)	$a'$ (fm)	$r_C$ (fm)
$d^a$	100	1.14	0.89	0	13.8	1.33	0.75	1.30
$t^a$	168	1.14	0.723	18.0	0	1.52	0.77	1.40
$^3\text{He}^b$	175	1.14	0.723	17.5	0	1.60	0.81	1.40
$\alpha^b$	206	1.41	0.519	25.8	0	1.41	0.519	1.30
bound $n$		1.25	0.65					1.25

<sup>a</sup> See Ref. 11.

<sup>b</sup> See Ref. 12.

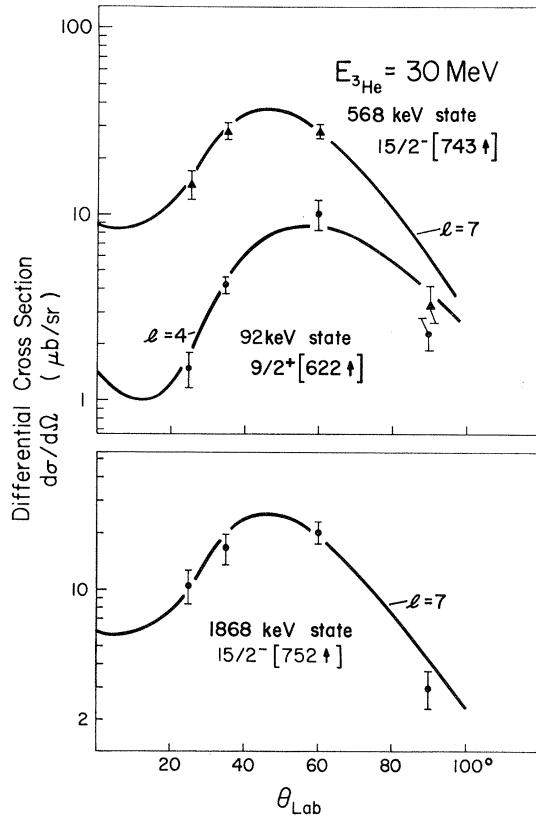


FIG. 3. Angular distributions of three  $\alpha$  groups measured in the  $^{242}\text{Pu}({}^3\text{He}, \alpha)$  reaction. The solid curves are the results of DWBA calculations using the optical-model parameters given in Table II.

assigned to the  $\frac{5}{2}^+[622\uparrow]$ ,  $\frac{7}{2}^+[624\uparrow]$ , and  $\frac{1}{2}^+[631\uparrow]$  configurations can be described as relatively pure Nilsson states.

The enhanced spectroscopic factors and the small rotational parameter of  $A = 4.4$  keV of the  $[743\uparrow]$  band give evidence of Coriolis mixing. In the Nilsson model, the  $[743\uparrow]$  and  $[752\uparrow]$  single-neutron levels originate from the  $1j_{15/2}$  shell-model state and are predicted to be strongly coupled. Coriolis mixing between components of the  $1j_{15/2}$  state was recently found in actinide nuclei<sup>3, 17</sup> neighboring  $^{241}\text{Pu}$ , e.g.,  $^{235}\text{U}$  and  $^{237}\text{U}$ . Taking Coriolis mixing between the  $[743\uparrow]$  and  $[752\uparrow]$  rotational bands into account, spectroscopic factors for the  $\frac{15}{2}$  levels of these two bands are calculated to be 2.4 and 1.0, respectively. These numbers compare somewhat more favorably with experiment than those calculated for pure Nilsson configurations of Table IV. Agreement between calculated and experimental spectroscopic factors can probably be further improved by including in the mixing calculation also the  $\frac{9}{2}^- [734\uparrow]$  configuration which is predicted at an excitation energy compara-

TABLE III. Cross-section ratios  $R = d\sigma({}^3\text{He}, \alpha)/d\sigma(d, t)$ .

Assignment	$l_0$	$1000 \times R_{\text{exp}}$	$1000 \times R_{\text{theor}}$		
			$l_0 - 1$	$l_0$	$l_0 + 1$
$\frac{9}{2}^+ [622\uparrow]$	4	$36 \pm 8$	9	30	93
$\frac{9}{2}^+ [631\uparrow]$	4	$35 \pm 7$	11	37	114
$\frac{11}{2}^- [743\uparrow]$	5	$72 \pm 27$	40	123	324
$\frac{13}{2}^+ [631\uparrow]$	6	$\approx 360$	128	336	833
$\frac{15}{2}^- [743\uparrow]$	7	$622 \pm 120$	351	868	
$\frac{5}{2}^+ [631\uparrow]$	2	$8 \pm 2$	2	5	16
$\frac{9}{2}^+ [631\uparrow]$	4	$64 \pm 10$	17	55	165
$\frac{1}{2}^- [501\uparrow]$	1	$< 4$	1	2	5
$\frac{9}{2}^+ [633\uparrow]$	4	$64 \pm 16$	25	62	186
$\frac{15}{2}^- [752\uparrow]$	7	$> 1000$	631	1533	

ble to that of the  $\frac{7}{2}^- [743\uparrow]$  state. Although the  $[734\uparrow]$  configuration is a particle state in  $^{241}\text{Pu}$  and the Coriolis matrix element with the  $[743\uparrow]$  state is reduced<sup>18</sup> due to pairing effects, mixing may still be considerable because of the small energy difference between these two configurations. The  $[734\uparrow]$  band has not yet been found experimentally in  $^{241}\text{Pu}$ , however, and therefore, a more detailed Coriolis calculation is unfeasible at present.

The assignment of the  $[501\uparrow]$  band is based on the good agreement of relative spectroscopic factors with theory. Rotational levels based on the  $[501\uparrow]$  configuration were recently identified<sup>19</sup> in  $^{239}\text{Pu}$  and in Th and U isotopes,<sup>20, 21</sup> having energy spacings and relative spectroscopic factors similar to those in  $^{241}\text{Pu}$ . On an absolute basis, however, the experimental spectroscopic factor of the  $\frac{1}{2}^- [501\uparrow]$  level in  $^{241}\text{Pu}$  is only about 35% of the predicted magnitude, suggesting strong fragmentation of the  $[501\uparrow]$  strength. Various vibrational excitations are found at energies as low as about 600 keV in this mass region,<sup>22</sup> and appreciable mixing between single-particle states and vibrations may occur. It is interesting to note that the  $\frac{1}{2}^- [501\uparrow]$  state is excited<sup>20</sup> with 82% of its theoretical strength at 558 keV in  $^{231}\text{Th}$ , and with 61% of the predicted strength at 869 keV in  $^{237}\text{U}$ . This observed tendency of the  $\frac{1}{2}^- [501\uparrow]$  state to become more fragmented with increasing energy lends added support to the present assignment of the  $\frac{1}{2}^- [501\uparrow]$  configuration.

Experimental spectroscopic factors of the rotational band based on the 809-keV level agree reasonably well with those calculated for the  $[631\uparrow]$  state. Therefore, the  $[631\uparrow]$  Nilsson configuration is tentatively assigned to this band. At 1181 keV a strong  $l=4$  transition is observed which may correspond to the  $\frac{9}{2}^+$  level of the  $[633\uparrow]$  rotational band. The spectroscopic factor of this level is about

TABLE IV. Observed and calculated spectroscopic factors.

State	$V^2$	Spectroscopic factor (Ref. a)			State	$V^2$	Spectroscopic factor (Ref. a)		
		Calculated	Observed ( $^3\text{He}, \alpha$ ) ( $d, t$ )				Calculated	Observed ( $^3\text{He}, \alpha$ ) ( $d, t$ )	
$\frac{5}{2}^+$ [622 $\uparrow$ ]	0.6	0.06	0	0.06	$\frac{7}{2}^-$ [743 $\uparrow$ ]	0.9	0		
$\frac{7}{2}^+$	0.6	0	0	0	$\frac{9}{2}^-$	0.9	0		
$\frac{9}{2}^+$	0.6	0.77	1.14	0.93	$\frac{11}{2}^-$	0.9	0.13	0.18	0.29
$\frac{11}{2}^+$	0.6	0.30	$\approx 0.2^b$	$\approx 0.2^b$	$\frac{13}{2}^-$	0.9	0.01		
$\frac{13}{2}^+$	0.6	0.07	0.17 <sup>b</sup>		$\frac{15}{2}^-$	0.9	1.66	2.52	3.26
$\frac{7}{2}^+$ [624 $\uparrow$ ]	0.2 <sup>c</sup>	0.02			$\frac{5}{2}^-$ [752 $\uparrow$ ]	1.0	0		
$\frac{9}{2}^+$	0.2	0.04			$\frac{7}{2}^-$	1.0	0.01		
$\frac{11}{2}^+$	0.2	0.33	0.41	$\approx 0.2$	$\frac{9}{2}^-$	1.0	0		
$\frac{13}{2}^+$	0.2	0.01			$\frac{11}{2}^-$	1.0	0.23		
$\frac{1}{2}^+$ [631 $\uparrow$ ]	0.8	0.20	0.13 <sup>b</sup>	0.12 <sup>b</sup>	$\frac{13}{2}^-$	1.0	0.01		
$\frac{3}{2}^+$	0.8	0.47	0.31 <sup>b</sup>	0.29 <sup>b</sup>	$\frac{15}{2}^-$	1.0	1.75	1.51	
$\frac{5}{2}^+$	0.8	0.06	0.08 <sup>b</sup>	0.04	$\frac{3}{2}^+$ [631 $\uparrow$ ]	1.0	0		0.08
$\frac{7}{2}^+$	0.8	0.17	0.40 <sup>b</sup>	0.16	$\frac{5}{2}^+$	1.0	0.24	( $\approx 0.7$ )	0.44
$\frac{9}{2}^+$	0.8	0.31	0.52	0.52	$\frac{7}{2}^+$	1.0	0.05	( $\approx 0.3$ )	( $\approx 0.1$ )
$\frac{11}{2}^+$	0.8	0.35			$\frac{9}{2}^+$	1.0	0.81	0.59	0.50
$\frac{13}{2}^+$	0.8	0.04	0.19	0.16	$\frac{11}{2}^+$	1.0	0.76	0.47	
$\frac{1}{2}^-$ [501 $\uparrow$ ]	1.0	1.30		0.46	$\frac{13}{2}^+$	1.0	0.14		
$\frac{3}{2}^-$	1.0	0.30		0.16 <sup>b</sup>	$\frac{5}{2}^+$ [633 $\uparrow$ ]	1.0	0.04		
$\frac{5}{2}^-$	1.0	0.33		0.18 <sup>b</sup>	$\frac{7}{2}^+$	1.0	0.23		
$\frac{7}{2}^-$	1.0	0.04			$\frac{9}{2}^+$	1.0	0.33	0.88	0.91
$\frac{9}{2}^-$	1.0	0.02			$\frac{11}{2}^+$	1.0	1.29	unobserved	unobserved
$\frac{11}{2}^-$	1.0	0			$\frac{13}{2}^+$	1.0	0.11		

<sup>a</sup>For the definition of the spectroscopic factor, see text.

<sup>b</sup>Extracted from unresolved group of lines by dividing the total intensity in the same ratio as the theoretical differential cross sections.

<sup>c</sup>Particle configuration.

three times as large as theoretically predicted, and a similar enhancement had recently been observed<sup>17, 20</sup> in  $^{237}\text{U}$ . In Refs. 17 and 20, the large spectroscopic factor of the  $\frac{9}{2}^+$ [633 $\downarrow$ ] state had been accounted for by Coriolis coupling between the [631 $\uparrow$ ] and [633 $\downarrow$ ] configurations. In disagreement with the experimental findings for  $^{237}\text{U}$  and the calculation of spectroscopic factors including band mixing, however, is the fact that in  $^{241}\text{Pu}$  the  $\frac{11}{2}^-$  level of the [633 $\downarrow$ ] band is not observed. The complete depletion of the  $\frac{11}{2}^+$ [633 $\downarrow$ ] strength cannot be explained with a simple two-band Coriolis coupling, inasmuch as the  $\frac{11}{2}^+$ [631 $\uparrow$ ] level does not show the corresponding strong enhancement. For these reasons, the assignment of the  $\frac{9}{2}^+$ [633 $\downarrow$ ] level should be regarded as very tentative. Additional experi-

mental data is necessary to positively identify the [633 $\downarrow$ ] rotational band and elucidate its detailed structure.

#### ACKNOWLEDGMENT

The authors wish to thank the operating crew of the tandem accelerator for generous cooperation. Thanks are also due G. W. Korn for the development of the emulsion plates, and Mrs. P. Hall for her careful plate scanning. Finally, the support of the Nuclear Structure Research Laboratory by the National Science Foundation is gratefully acknowledged.

\*Work supported by the U. S. Atomic Energy Commission.

- <sup>1</sup>G. R. Satchler, *Ann. Phys. (N.Y.)* **3**, 275 (1958).  
<sup>2</sup>T. H. Braid, R. R. Chasman, J. R. Erskine, and A. M. Friedman, *Phys. Letters* **18**, 149 (1965).  
<sup>3</sup>Th. W. Elze and J. R. Huizenga, *Nucl. Phys.* **A133**, 10 (1969).  
<sup>4</sup>Th. W. Elze and J. R. Huizenga, *Phys. Rev. C* **1**, 328 (1970).  
<sup>5</sup>E. K. Hyde, I. Perlman, and G. T. Seaborg, *The Nuclear Properties of the Heavy Elements* (Prentice-Hall, Inc., Englewood Cliffs, New Jersey, 1964).  
<sup>6</sup>C. M. Lederer, J. M. Hollander, and I. Perlman, *Table of Isotopes* (John Wiley & Sons, Inc., New York, 1967), 6th ed.  
<sup>7</sup>Th. W. Elze and J. R. Huizenga, *Bull. Am. Phys. Soc.* **15**, 547 (1970).  
<sup>8</sup>The target was supplied by the U. S. Atomic Energy Commission through the Isotopes Division of Oak Ridge National Laboratory, Oak Ridge, Tennessee.  
<sup>9</sup>R. H. Bassel, R. M. Drisko, and G. R. Satchler, Oak Ridge National Laboratory Report No. ORNL-3240, 1962 (unpublished).  
<sup>10</sup>Supplied by P. Kunz of the University of Colorado.  
<sup>11</sup>G. Muehlechner, A. S. Poltorak, and W. C. Parkinson,

- Phys. Rev.* **159**, 1039 (1967).  
<sup>12</sup>G. R. Satchler, private communication.  
<sup>13</sup>R. Stock, R. Bock, P. David, H. H. Duhm, and T. Tamura, *Nucl. Phys.* **A104**, 136 (1967).  
<sup>14</sup>R. H. Bassel, *Phys. Rev.* **149**, 791 (1966).  
<sup>15</sup>J. P. Davidson, *Collective Models of the Nucleus* (Academic Press Inc., New York, 1968).  
<sup>16</sup>O. Nathan and S. G. Nilsson, in *Alpha-, Beta-, and Gamma-Ray Spectroscopy*, edited by K. Siegbahn (North-Holland Publishing Company, Amsterdam, The Netherlands, 1965).  
<sup>17</sup>T. v. Egidy, Th. W. Elze, and J. R. Huizenga, *Nucl. Phys.* **A145**, 306 (1970).  
<sup>18</sup>P. O. Tjøm and B. Elbek, *Kgl. Dansk Vidensk. Selskab, Mat.-Fys. Medd.* **36**, No. 8 (1967).  
<sup>19</sup>D. W. Davies and J. M. Hollander, *Nucl. Phys.* **68**, 161 (1965).  
<sup>20</sup>J. S. Boyno, Th. W. Elze, and J. R. Huizenga, to be published.  
<sup>21</sup>T. H. Braid, R. R. Chasman, J. R. Erskine, and A. M. Friedman, *Phys. Rev. C* **1**, 275 (1970).  
<sup>22</sup>M. R. Schmorak, C. E. Bemis, Jr., M. Zender, F. E. Coffman, A. V. Ramayya, and J. H. Hamilton, *Phys. Rev. Letters* **24**, 1507 (1970).

## Experimental Test of the Kumar-Baranger Pairing-Plus-Quadrupole Force Model in the $A = 190$ Region Through $E2/M1$ Mixing Amplitudes\*

K. S. Krane† and R. M. Steffen

*Department of Physics, Purdue University, Lafayette, Indiana 47907*

(Received 18 August 1970)

The  $E2/M1$  multipole mixing ratios  $\delta(\gamma)$  of  $\gamma$  transitions in even-even osmium and platinum isotopes have been measured in order to test the predictions of the pairing-plus-quadrupole theory of Kumar and Baranger. The mixing ratios  $\delta(\gamma)$  were determined from directional-correlation measurements on  $\gamma$  transitions in  $^{186,188,190}\text{Os}$  (populated in the decay of  $^{186,188,190}\text{Ir}$  and in  $^{194,196}\text{Pt}$  (populated in the decay of  $^{194,196}\text{Au}$ )). The radioactive iridium isotopes were produced by  $\text{Re}(\alpha, xn)$  reactions, and the gold isotopes were produced by  $\text{Pt}(d, xn)$  reactions. The equipment employed for the  $\gamma$ - $\gamma$  directional-correlation measurements consisted of two coaxial 30-cc Ge(Li) detectors and appropriate electronic equipment for high-resolution pulse-height analysis and timing analysis. The observed directional correlations were analyzed in terms of the appropriate  $E2/M1$  mixing ratios, which are defined explicitly. The following results were obtained (predictions of the Kumar-Baranger theory are listed in square brackets):  $\delta(^{186}\text{Os}, 630 \text{ keV}) = -(10^{+15}) [-14.7]$ ,  $\delta(^{186}\text{Os}, 773 \text{ keV}) = -(13^{+9}) [-13.5]$ ,  $\delta(^{188}\text{Os}, 478 \text{ keV}) = -12.3 \pm 2.6 [-9.5]$ ,  $\delta(^{188}\text{Os}, 635 \text{ keV}) = -6.9 \pm 3.2 [-10.5]$ ,  $\delta(^{190}\text{Os}, 371 \text{ keV}) = -8.5 \pm 1.0 [-7.6]$ ,  $\delta(^{190}\text{Os}, 569 \text{ keV}) = -9.0 \pm 1.5 [-9.9]$ ,  $\delta(^{194}\text{Pt}, 293 \text{ keV}) = +14.3 \pm 2.1 [+19.9]$ ,  $\delta(^{196}\text{Pt}, 333 \text{ keV}) = -5.7 \pm 0.3 [-101.4]$ . Except for the 333-keV transition in  $^{196}\text{Pt}$  the agreement of the experimental mixing ratios with the values and signs predicted by the Kumar-Baranger model is excellent.

### I. INTRODUCTION

The nuclei of the osmium and platinum isotopes are situated in a transition region between the nuclei possessing large equilibrium deformations in the range  $150 < A < 180$  and the spherical nuclei near the doubly magic  $^{208}\text{Pb}$ . Knowledge of the

static and dynamic properties of the excited states of such nuclei would provide insight into the details of their structure, and would provide a basis for the evaluation of various microscopic and phenomenological nuclear models.

In recent years, much effort has been expended in the study of energy levels, electromagnetic mul-